Journal of Molecular Catalysis B: Enzymatic 66 (2010) 55–62

Contents lists available at ScienceDirect

Journal of Molecular Catalysis B: Enzymatic

journal homepage: www.elsevier.com/locate/molcatb

Kinetic resolution of a drug precursor by *Burkholderia cepacia* lipase immobilized by different methodologies on superparamagnetic nanoparticles

Leandro H. Andrade[a,*], Lya P. Rebelo[a], Caterina G.C.M. Netto[b], Henrique E. Toma[b]

[a] *Laboratory of Fine Chemistry and Biocatalysis, Institute of Chemistry, University of São Paulo, CEP 05508-900, São Paulo, SP, Brazil*
[b] *Supramolecular NanotechLab, Institute of Chemistry, University of São Paulo, CEP 05508-900, São Paulo, SP, Brazil*

ARTICLE INFO

Article history:
Received 15 December 2009
Received in revised form 9 March 2010
Accepted 10 March 2010
Available online 20 March 2010

Keywords:
Lipase
Kinetic resolution
Superparamagnetic nanoparticles
Burkholderia cepacia lipase
Chiral drug

ABSTRACT

Burkholderia cepacia lipase was immobilized on superparamagnetic nanoparticles using three different methodologies (adsorption, chemisorption with carboxibenzaldehyde and chemisorption with glutaraldehyde) and employed in the kinetic resolution of a chiral drug precursor, (*RS*)-2-bromo-1-(phenyl)ethanol, *via* enantioselective acetylation reaction. An excellent improvement of lipase catalytical performance was observed. Free *B. cepacia* lipase gave the ester (*S*)-**2** with poor *E*-value <30, and after its immobilization to magnetic nanoparticles the *E*-value was up to >200. The effect of several reaction parameters in the kinetic resolution was studied. The best results for kinetic resolution were obtained using vinyl acetate as acetyl donor and toluene as solvent, typically yielding the ester in high enantiomeric excess (>99%) and *E*-value (*E* > 200). Of the three tested immobilization methods, chemisorption with glutaraldehyde was the best one in terms of temperature stability and yield product.

1. Introduction

The use of lipases as catalysts is contributing to the rise of the exciting and rapidly growing area of chiral organic synthesis [1–10]. As a matter of fact, research in this area is pursuing the discovery of new efficient enzymes, new target compounds, and also of new convenient solid supports, capable of sustaining the enzymatic activity in organic media with minimum loss. In particular, the immobilization of enzymes on magnetic particles is viewed as a very attractive strategy, for allowing their separation and recovery from the reaction media by the simple use of a magnet [11–15]. On the other hand, the reusability of the immobilized enzymes represents an outstanding green-chemistry approach, reducing the cost and amount of such expensive biocatalysts. It should be noticed that superparamagnetic nanoparticles exhibit a single magnetic domain in their nanocrystalline structures, and this is responsible for their exceptional magnetization properties in the presence of a magnetic field. A suitable superparamagnetic species is based on magnetite (γ-Fe_3O_4). Large surface area, high mass transference and rapid response to external magnetic fields are remarkable characteristics ennobling this type of nanometric support or carrier. In addition, enzyme immobilization on superparamagnetic nanoparticles can permit the recovery of the biocatalyst without spending energy, by using permanent magnets.

Recently, *Burkholderia cepacia* lipase (BCL, also known as *Pseudomonas cepacia* lipase) has been employed as biocatalyst in a variety of synthetic applications, performing reactions, such as hydrolysis [16–18], enantioselective acylation [19] and transesterification [20–23]. In view of the wide usefulness of *P. cepacia* lipase, the possibility of exploring its recyclability using superparamagnetic nanoparticles may be quite rewarding. For this reason, a detailed study focusing on the immobilization of this lipase on superparamagnetic nanoparticles was carried out, aiming its application in the kinetic resolution of the chiral drug precursor, (*RS*)-2-bromo-1-(phenyl)ethanol. This compound is envisaged as a common building block to the chiral compounds Fluoxetine, Tomoxetine and Nisoxetine [24–26], which are among the most important pharmaceuticals for the treatment of psychiatric disorders (depression, anxiety, alcoholism) and also metabolic problems (obesity and bulimia).

2. Results and discussion

Immobilization of enzymes at superparamagnetic nanoparticles involves specific molecular interactions at the surface, and can induce some structural reorganization, thus changing the behavior of the catalytic sites. Therefore, a comparative study was carried out in this work, by immobilizing the lipase according to three different procedures. Initially, magnetite (Fe_3O_4) nanoparticles (MagNP) were prepared by the co-precipitation method, mixing Fe^{3+} and

* Corresponding author.
E-mail addresses: leandroh@iq.usp.br (L.H. Andrade), henetoma@iq.usp.br (H.E. Toma).

1381-1177/$ – see front matter © 2010 Elsevier B.V. All rights reserved.
doi:10.1016/j.molcatb.2010.03.002

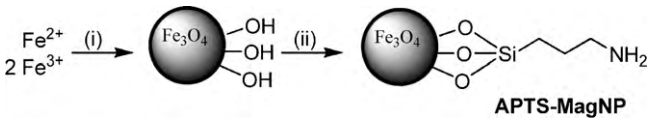

Scheme 1. (i) Co-precipitation of Fe^{2+} and Fe^{3+} oxides in alkaline solution; (ii) silanization of the Fe_3O_4 nanoparticles with APTS.

Fe^{2+} ions in NaOH solution, under an argon atmosphere. In order to eliminate any possible interference from the iron-oxide/hydroxide sites in the catalytic process, and to promote a better nanoparticles protection against air oxidation, a silanization treatment was applied, using γ-aminopropyltriethoxysilane (APTS), as shown in Scheme 1. The resulting black material exhibited strong magnetization in the presence of a magnetic field. Transmission electron microscopy revealed the presence of nearly cubic particles, exhibiting an average core size of 10 nm [27]. The silanization treatment provides a stable silicate coating by forming strong Fe–O–Si and cross-linked Si–O–Si bonds, leaving the γ-aminopropyl groups available for interacting with external species, protons, metal ions and solvent molecules. At neutral or slightly acidic solutions, the APTS amino groups are protonated ($pK_a = 9$), yielding a net positive charge responsible for the stabilization of the colloidal solutions.

The first immobilization procedure consisted in the direct interaction of lipase with the APTS modified superparamagnetic nanoparticles (APTS-MagNP). In spite of its rather simple nature, the direct interaction of the enzyme with the functionalized nanoparticles surface is driven by adsorption, proceeding according to a Langmuir isotherm which depends on many parameters, including the relative amounts of the interacting species, temperature and time. In this work, by using the same concentration of *B. cepacia* lipase (0.55 mg/mL) at 32 °C, the amount of APTS-MagNP was varied from 10 to 30 mg. The extent of enzyme binding was quantified using Bradford's method [28] after 3 successive washings. A typical analysis indicated the presence of 0.21 mg of protein bound to 20 mg of APTS-MagNP, a result consistent with a relatively strong enzyme–nanoparticle interaction. It can involve hydrogen bonding formation and electrostatic interactions, since at pH 7, *B. cepacia* lipase has a negative charge (isoelectric point = 5.2) [29] and the magnetic nanoparticles exhibit a positive charge due to the protonation of the aliphatic amino group [30]. In addition, there are also many amide and aminoacid residues in this lipase available for interacting with the proton.

In the second procedure, immobilization of *B. cepacia* lipase on superparamagnetic nanoparticles was carried out chemically through the formation of a covalent link, after the modification of APTS-MagNP with 4-carboxybenzaldehyde (Scheme 2). In this procedure, the amino group of APTS reacts with aldehyde, forming an imine intermediate, which is then reduced with $NaBH_4$, along with the remaining aldehyde groups, to give a carboxy-substituted species (Carboxy-APTS-MagNP). Thus, the lipase can be covalently bound to the carboxy-substituted species *via* carbodiimide activation. This step involves the conversion of the carboxyl group into an active ester by reacting with EDC (1-ethyl-3-(3-dimethyl aminopropyl) carbodiimide hydrochloride), allowing the binding of the lipase to afford the biocatalyst named as BCL-Carboxy-APTS-MagNP.

By using this methodology, it was possible to bind 0.25 mg of protein to 20 mg of Carboxy-APTS-MagNP, quantified by Bradford method.

In the third procedure, *B. cepacia* lipase was immobilized onto the superparamagnetic nanoparticles using glutaraldehyde to afford the biocatalyst named as BCL-Glu-APTS-MagNP (Scheme 3). The role of glutaraldehyde is to react with the amino group of APTS, forming an imine bond and leaving another terminal aldehyde group for reacting with the amino residues of the enzyme, as shown in Scheme 3.

A typical amount of lipase immobilized by this methodology was 0.28 mg of protein to 20 mg of Glu-APTS-MagNP, quantified by Bradford method.

2.1. Topographic analysis

B. cepacia lipase immobilized onto APTS-MagNPs, seems to form extensive conglomerates when it was deposited at a flat mica surface, as can be seen in the AFM topographic and phase contrast imaging shown in Fig. 1. The conglomerate images are reproduced in the magnetic force microscopy (Fig. 1C) confirming their magnetic nature. Similar images were observed for the immobilized enzymes prepared by the several methods.

The conglomerate profiles are better seen in the 3D and cross-diagonal scan images, shown in Fig. 2. They actually appear like islands about 500 nm wide, composed by agglomerated nanoparticles. However, it should be noticed that the typical AFM images of APTS-MagNP exhibit a rather uniform distribution of nanoparticles all over the flat mica surface (Fig. 3). Therefore, the formation of such conglomerates, instead of a random distribution of the particles, indicates that the enzyme is facilitating their agglomeration onto the flat mica surface, during the drying process.

2.2. FTIR vibrational analysis

Typical FTIR spectra of the magnetic nanoparticles (MagNP) and their APTS modified forms (Fig. 4), as well as of the free *B. cepacia* lipase and their immobilized forms were superimposed in Fig. 5, for comparison purposes. The strong peaks at 585 and 632 cm^{-1} in the magnetic nanoparticles correspond to the ν(Fe–O) vibrational mode characteristic of bulk magnetite [31–34]. The silica network is adsorbed on the magnetite surface by Fe–O–Si bonds, and the corresponding infrared signals are usually overlapped with

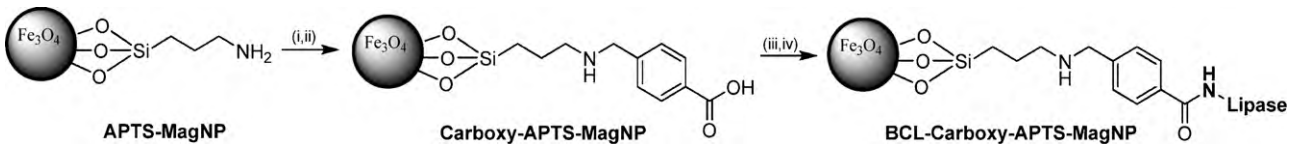

Scheme 2. (i) 4-Carboxybenzaldehyde, 4 h; (ii) $NaBH_4$, 1 h; (iii) EDC, 20 min; (iv) *Burkholderia cepacia* lipase, 1 h.

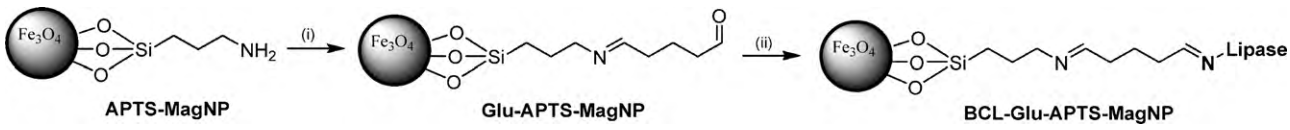

Scheme 3. (i) Glutaraldehyde; (ii) *B. cepacia* lipase.

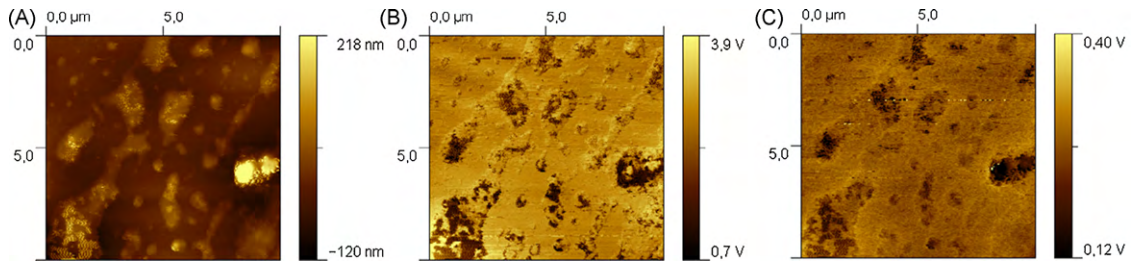

Fig. 1. Atomic force microscopy of lipase from *B. cepacia* immobilized *via* glutaraldehyde method on magnetic nanoparticles: (A) topography, (B) phase contrast and (C) magnetic force microscopy.

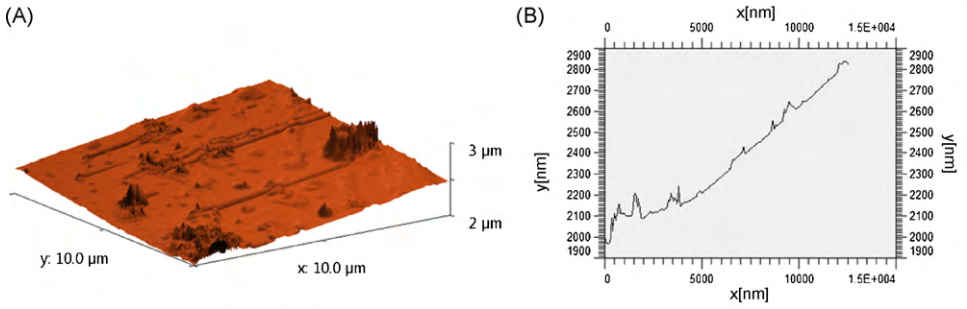

Fig. 2. (A) 3D view of the atomic force microscopy of lipase from *B. cepacia* immobilized *via* glutaraldehyde method on magnetic nanoparticles and (B) a diagonal scan showing the specific roughness.

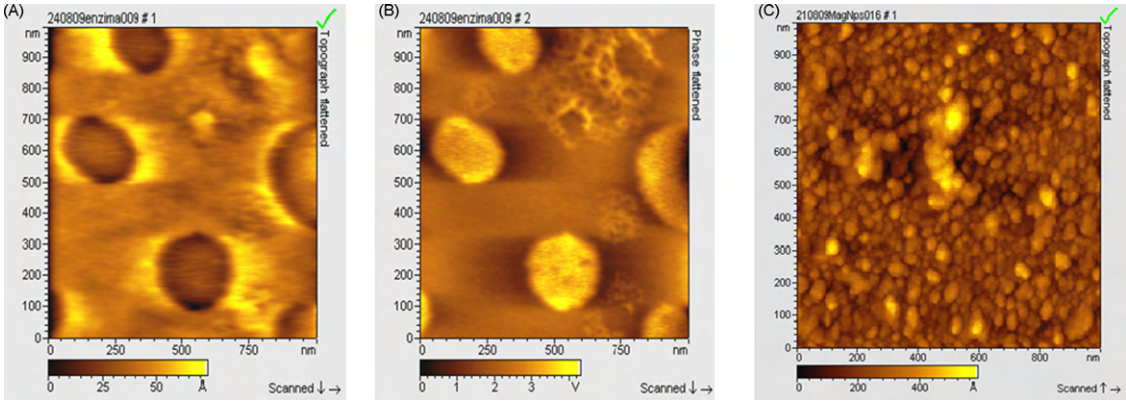

Fig. 3. Atomic force microscopy of (A) topography and (B) phase contrast of a free lipase from *B. cepacia* film, and (C) topography of magnetic nanoparticles film (APTS-MagNP).

the Fe–O band of magnetite. The silane polymer onto the surface of magnetite particles is responsible for the broad vibrational band at 1100–900 cm^{-1}, assigned to the Si–O–H and Si–O–Si groups. The weak bands at 3417 and 1625 cm^{-1} are ascribed to the N–H stretching and H–N–H bending modes of the free/protonated amino group, respectively [35,36]. Hydrogen-bonded silanols also absorb around 3200 and 3470 cm^{-1} [35,37].

The FTIR spectrum of *B. cepacia* lipase shows the characteristic amide I [38] band at 1652 cm^{-1}, while the amide II band appears around 1568 cm^{-1}. The amide III and IV bands are observed at 1285 and 726 cm^{-1}. The vibrational peaks around 1100–1000 cm^{-1} are associated with the C–C and C–N composite vibrations of the protein chain.

When *B. cepacia* lipase is immobilized onto APTS-MagNP (Fig. 5A) there is a strong overlap of the vibrational peaks of the enzyme and nanoparticles. The amide I band appears at 1635 cm^{-1}. The observed shift has been associated with an increase in the inter- and intramolecular β-structure and a decrease in the α-helix amount. This interchange of secondary structures can sometimes be observed in other nanoparticles–enzyme systems

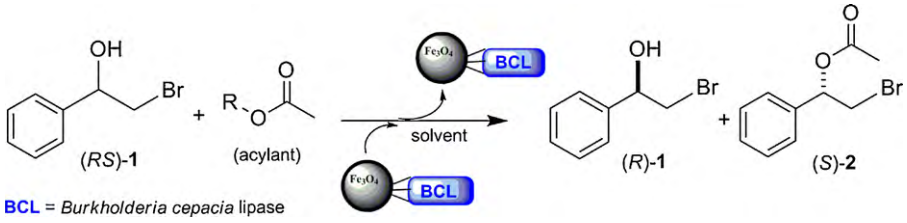

Scheme 4. Kinetic resolution of (*RS*)-2-bromo-1-(phenyl)ethanol (**1**) by *B. cepacia* lipase-catalyzed acetylation.

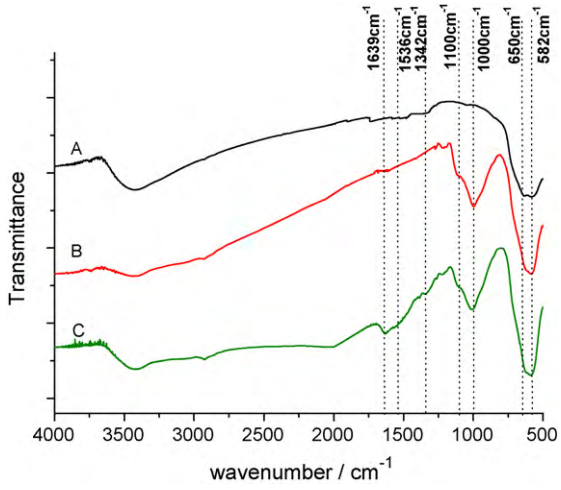

Fig. 4. Infrared spectra of (A) nude magnetic nanoparticles (MagNP), (B) silanized magnetic nanoparticles (APTS-MagNP) and (C) magnetic nanoparticles functionalized with carboxybenzaldehyde (Carboxy-APTS-MagNP).

[39]. The characteristic amide II band is shifted to 1557 cm^{-1}. The amide II position is sensitive to the environment around the protein. Its shift to lower wavenumbers seems to reflect the immobilization and possible structural changes. In addition, there is strong enhancement of the vibrational peaks in the 1500–900 cm^{-1} region, involving the amide III, the skeletal C–C, C–N, and Si–O vibrations. Although a detailed assignment is not possible at the present time because of the complexity involved, the observed changes in the vibrational spectra corroborate the existence of different binding modes of the enzyme to the magnetic nanoparticles.

2.3. Enzyme activity: kinetic resolution of (RS)-2-bromo-1-(phenyl)ethanol

The lipase activity for each immobilization method was evaluated in the kinetic resolution (KR) of a chiral drug precursor (*RS*)-2-bromo-1-(phenyl)ethanol (**1**) *via* enantioselective acetylation reaction (Scheme 4).

Typical results obtained for the free *B. cepacia* lipase, are shown in Table 1, and will be taken as reference for comparison purposes with respect to the catalytic activity of the immobilized enzyme (Table 1). As we employed a lipase solution in the immobilization

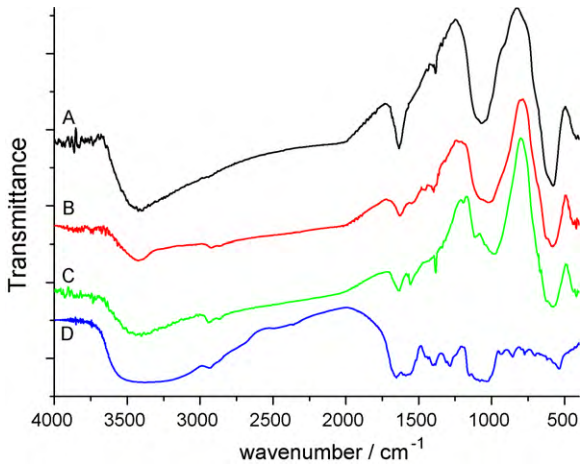

Fig. 5. Infrared spectra of (A) lipase from *B. cepacia* adsorbed on APTS-MagNP, (B) lipase immobilized onto magnetic nanoparticles by carboxybenzaldehyde method (Carboxy-APTS-MagNP), (C) lipase immobilized with glutaraldehyde and (D) free lipase from *B. cepacia*.

Table 1
Kinetic resolution of (*RS*)-2-bromo-1-(phenyl)ethanol by free *B. cepacia* lipase-catalyzed acetylation.[a].

Entry	Solvent	Time (h)	*ee* (%)[b]		Conv. (%)[c]	*E*[d]
			(*R*)-**1**	(*S*)-**2**		
1	TBME	5	2	30	5	<30
2	TBME	24	3	45	6	<30
3	Toluene	5	10	70	12	<30
4	Toluene	24	20	78	20	<30

[a] General conditions: (*RS*)-2-bromo-1-(phenyl)ethanol (0.01 mmol), lipase (16 mg), vinyl acetate (30 μL), solvent (1 mL), 32 °C, 800 rpm.
[b] *ee* = enantiomeric excess was determined by chiral GC analysis.
[c] Conv. = conversion = $ee_S/(ee_S + ee_P)$.
[d] $E = \{\ln[ee_P(1 - ee_S)]/(ee_P + ee_S)\}/\{\ln[ee_P(1 + ee_S)]/(ee_P + ee_S)\}$ [40,41].

studies, we prepared a lyophilized form of *B. cepacia* lipase from this enzymatic solution to be used in the kinetic resolution of (*RS*)-2-bromo-1-(phenyl)ethanol.

As one can see in Table 1, the reactions using free *B. cepacia* lipase in different solvents and reaction time afforded the ester **2** with very low *E*-value, low conversion and poor enantiomeric excess of ester.

Similar experiments were carried out using the enzyme immobilized onto the magnetic nanoparticles, according to three different procedures. Initially, we evaluated the influence of different acyl donor nature, solvent, and reaction time for the enantioselective acetylation of (*RS*)-**1** catalyzed by lipase immobilized onto magnetic nanoparticles using adsorption method (BCL-APTS-MgNP). In this study, we employed vinyl acetate, isoprenyl acetate and ethyl acetate, in two different solvents (*tert*-butyl methyl ether = TBME and toluene). The results are shown in Table 2 (entries 1–6).

Among the acyl donor evaluated, ethyl acetate did not afford the ester **2** in both solvents (Table 2, entries 3 and 6). However, vinyl acetate showed to be a better acyl donor than isoprenyl acetate in terms of conversion (Table 2, entries 1 and 4). When one compares the reactions using toluene and TBME as solvent, a little difference in conversion was observed (Table 2, entries 1 and 4; 2 and 5). The *E*-values in all cases were higher than 200, which indicated an excellent enantioselectivity. As shown in Table 1, KR of (*RS*)-**1** catalyzed by free *B. cepacia* lipase gave the ester (*S*)-**2** with poor *E*-value, and now, by the simple immobilization of this lipase to magnetic nanoparticles the *E*-value was up to >200, which indicated a excellent improvement of the catalytical performance of the *B. cepacia* lipase.

In view of these results, vinyl acetate was selected as the acyl donor to be employed on the evaluation of the influence of reaction temperature and time in the enzymatic kinetic resolution of the (*RS*)-2-bromo-1-(phenyl)ethanol (Table 2, entries 7–12). We carried out the acetylation reaction at temperatures varying from 32 to 52 °C using different reaction times (24, 48, and 72 h). The highest conversion was obtained with the reaction temperature maintained at 42 °C after 24 h (Table 2, entry 9). However, at the same temperature, an increase in reaction time resulted a decreased of conversion occurred probably due to a desorption process, typical when the lipase is immobilized by adsorption method. In spite of this, the adsorption method can be a good option to immobilize *B. cepacia* lipase onto magnetic nanoparticles, since this protocol is much easier to handle.

The activities of the *B. cepacia* lipase immobilized *via* glutaraldehyde and carboxybenzaldehyde methods on magnetic nanoparticles were also determined in the KR of (*RS*)-2-bromo-1-(phenyl)ethanol. The results are shown in Table 3.

Initially, we evaluated the acyl donor and solvent for KR of (*RS*)-**1** (Table 3, entries 1–6 and 13–18). When ethyl acetate was used as acyl donor, the ester **2** was not obtained by any immobilized form of *B. cepacia* lipase (Table 3, entries 3, 6, 15 and 18). Once again,

Table 2
KR of (*RS*)-2-bromo-1-(phenyl)ethanol *via* enantioselective acetylation catalyzed by *B. cepacia* lipase immobilized onto magnetic nanoparticles using adsorption method.[a]

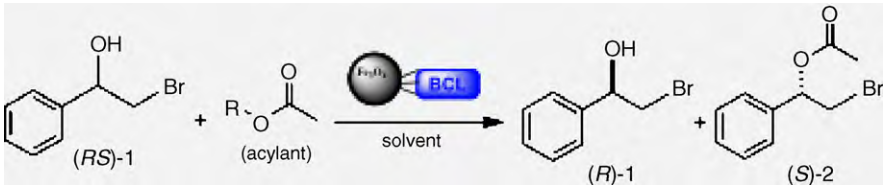

Entry	*T* (°C)	Time (h)	Acylant	Solvent	*ee* (%)[b]		Conv. (%)[c]	*E*[d]
					(*R*)-**1**	(*S*)-**2**		
1	32	24	Vinyl acetate	TBME	11	>99	10	>200
2	32	24	Isoprenyl acetate	TBME	3	>99	4	>200
3	32	24	Ethyl acetate	TBME	–	–	–	–
4	32	24	Vinyl acetate	Toluene	15	>99	13	>200
5	32	24	Isoprenyl acetate	Toluene	6	>99	5	>200
6	32	24	Ethyl acetate	Toluene	–	–	–	–
7	32	48	Vinyl acetate	Toluene	23	>99	19	>200
8	32	72	Vinyl acetate	Toluene	21	>99	17	>200
9	42	24	Vinyl acetate	Toluene	51	>99	34	>200
10	42	48	Vinyl acetate	Toluene	16	>99	14	>200
11	52	24	Vinyl acetate	Toluene	14	>99	12	>200
12	52	48	Vinyl acetate	Toluene	10	>99	9	>200

(–) = no reaction.
[a] General conditions: (*RS*)-2-bromo-1-(phenyl)ethanol (0.01 mmol), acylant (30 μL), solvent (1 mL), lipase (0.21 mg/20 mg APTS-MgNP), 800 rpm.
[b] *ee* = enantiomeric excess was determined by chiral GC analysis.
[c] Conv. = conversion = $ee_S/(ee_S + ee_P)$.
[d] $E = \{\ln[ee_P(1 - ee_S)]/(ee_P + ee_S)\}/\{\ln[ee_P(1 + ee_S)]/(ee_P + ee_S)\}$ [40,41].

vinyl acetate was the best acyl donor, and reactions using toluene and TBME as solvent showed a little difference in conversion but with excellent enantioselectivities (*E*-values >200, Table 3, entries 1, 4, 13, and 16).

KR of (*RS*)-**1** catalyzed by *B. cepacia* lipase immobilized *via* glutaraldehyde and carboxybenzaldehyde methods was performed at temperatures varying from 32 to 52 °C using different reaction time (Table 3, entries 7–12 and 19–24). In all cases, the *ee* product and *E*-values were excellent as observed with BCL immobilized by adsorption method (Table 2). These results indicate that different immobilization methods have no effect on the enzyme activity in terms of enantioselectivity. In case of the lipase immobilization by the carboxybenzaldehyde method (BCL-Carboxy-APTS-MagNP), the increase in reaction time from 24 to 48 h did not make a significant conversion improvement (Table 3, entries 1, 4, 7, and 8). In addition, the KR at 52 °C gave lower conversion than 42 °C indicating a small decay of enzyme activity caused by temperature (Table 3, entries 9–12). However, a good conversion (24%) was observed for enantioselective acetylation after 48 h at 42 °C (Table 3, entry 10).

The highest conversions for KR of (*RS*)-**1** were obtained with the lipase immobilized by the glutaraldehyde method (up to 34%; Table 3, entry 24). In addition, varying the temperature from 32 to 52 °C a linear increase in conversion was obtained (Table 3, entries 19–24). In this case, we can mention that both immobilized form of *B. cepacia* lipase via chemisorption showed very good efficiency at high temperature after 48 h reaction. These results can be attributed to the covalent binding of lipase to the magnetic nanoparticles (γ-aminopropyltriethoxysilane modified nanoparticles) which helps stabilizing the enzyme at high temperatures and long reaction time [42,43]. On the other hand, these results can also be affect by the protocol employed in the preparation of modified magnetic nanoparticles. The best results were obtained with *B. cepacia* lipase immobilized by the glutaraldehyde method, in which the lipase was easily treated with previously activated nanoparticles with glutaraldehyde. Meanwhile, in the preparation of BCL-Carboxy-APTS-MagNP it was employed different chemical reagents and reaction steps, then, a sharp decrease in enzyme stability can occur due to these chemical treatments.

2.4. Conclusion

B. cepacia lipase can be immobilized on magnetite by different methods, exhibiting good compatibility with the supporting material. An excellent improvement of lipase catalytical performance, as determined in the KR of (*RS*)-2-bromo-1-phenylethanol, was observed. Free *B. cepacia* lipase gave the ester (*S*)-**2** with poor *E*-value <30, and after its immobilization onto magnetic nanoparticles the *E*-value was up to >200. Immobilization *via* glutaraldehyde and carboxybenzaldehyde methods proved to be more effective for transesterification reactions in high temperatures (up to 52 °C).

3. Experimental

3.1. General methods

Amano Lipase PS from *B. cepacia* was purchased from Sigma–Aldrich. Solvents were purified by standard procedures. Some reagents are commercially available and were used without further purification. Thin-layer chromatography (TLC) was performed using pre-coated plates (Aluminum foil, Silica Gel 60 F254 Merck, 0.25 mm). Silica gel (0.035–0.070 mm, Acros) was used for column chromatography. GC analyses were performed in a Shimadzu GC-17A instrument with a FID detector, using hydrogen as a carrier gas (100 kPa). The GC chiral column used was a Chirasil-Dex CB β-cyclodextrin (25 m × 0.25 mm) for determination of the enantiomeric excesses. Low Resolution Mass Spectra (LRMS) were recorded on a Shimadzu GCMS P5050A (70 eV) spectrometer. Optical rotations were determined on a JASCO DIP-378 polarimeter. Infrared spectra were recorded on a Perkin–Elmer 1750-FT-IR spectrometer. NMR spectra were recorded on Varian Gemini-200 instrument. For NMR ^{1}H (instrument operating at 200 MHz, δ values are referenced to $(CH_3)_4Si$ (0 ppm) and for NMR ^{13}C (instrument operating at 50 MHz, δ values are referenced to $CDCl_3$ (77.0 ppm).

Table 3
Kinetic resolution of (*RS*)-2-bromo-1-(phenyl)ethanol *via* enantioselective acetylation catalyzed by *B. cepacia* lipase immobilized onto APTS-MagNP using carboxybenzaldehyde[a] and glutaraldehyde[b] method.

Entry	*T* (°C)	Time (h)	Acylant	Solvent	*ee* (%)[c]		Conv. (%)[d]	*E*[e]
					(*R*)-**1**	(*S*)-**2**		
1[a]	32	24	Vinyl acetate	TBME	15	>99	16	>200
2[a]	32	24	Isoprenyl acetate	TBME	34	>99	12	>200
3[a]	32	24	Ethyl acetate	TBME	–	–	–	–
4[a]	32	24	Vinyl acetate	Toluene	11	>99	10	>200
5[a]	32	24	Isoprenyl acetate	Toluene	7	>99	6	>200
6[a]	32	24	Ethyl acetate	Toluene	–	–	–	–
7[a]	32	48	Vinyl acetate	Toluene	17	>99	15	>200
8[a]	32	72	Vinyl acetate	Toluene	16	>99	14	>200
9[a]	42	24	Vinyl acetate	Toluene	21	>99	18	>200
10[a]	42	48	Vinyl acetate	Toluene	36	>99	24	>200
11[a]	52	24	Vinyl acetate	Toluene	20	>99	17	>200
12[a]	52	48	Vinyl acetate	Toluene	26	>99	21	>200
13[b]	32	24	Vinyl acetate	TBME	20	>99	17	>200
14[b]	32	24	Isoprenyl acetate	TBME	23	>99	18	>200
15[b]	32	24	Ethyl acetate	TBME	–	–	–	–
16[b]	32	24	Vinyl acetate	Toluene	23	>99	18	>200
17[b]	32	24	Isoprenyl acetate	Toluene	10	>99	9	>200
18[b]	32	24	Ethyl acetate	Toluene	–	–	–	–
19[b]	32	48	Vinyl acetate	Toluene	33	>99	25	>200
20[b]	32	72	Vinyl acetate	Toluene	40	>99	29	>200
21[b]	42	24	Vinyl acetate	Toluene	22	>99	18	>200
22[b]	42	48	Vinyl acetate	Toluene	38	>99	26	>200
23[b]	52	24	Vinyl acetate	Toluene	31	>99	24	>200
24[b]	52	48	Vinyl acetate	Toluene	50	>99	34	>200

(–) = no reaction; general conditions: (*RS*)-2-bromo-1-(phenyl)ethanol (0.01 mmol), acylant (30 μL), solvent (1 mL), lipase (carboxybenzaldehyde method = 0.25 mg lipase/20 mg APTS-MgNP, glutaraldehyde method = 0.28 mg lipase/20 mg APTS-MgNP), 800 rpm.

[a] BCL immobilized by carboxybenzaldehyde method.

[b] BCL immobilized by glutaraldehyde method.

[c] *ee* = enantiomeric excess was determined by chiral GC analysis.

[d] Conv. = conversion = $ee_S/(ee_S + ee_P)$.

[e] $E = \{\ln[ee_P(1 - ee_S)]/(ee_P + ee_S)\}/\{\ln[ee_P(1 + ee_S)]/(ee_P + ee_S)\}$ [40,41].

Chemical shifts are given in ppm and coupling constants are given in Hertz (s = singlet, d = doublet, m = multiplet).

3.2. Synthesis of (RS)-2-bromo-1-(phenyl)ethanol (**1**)

In an one-necked round-bottomed flask, styrene (260 mg, 2.5 mmol) was dissolved in water (10 mL) and NBS (*N*-bromosuccinimide, 470 mg, 2.5 mmol). This mixture was stirred vigorously at room temperature until the solid NBS disappeared (35 min). The resulting solution was extracted with CH_2Cl_2 (3× 10 mL). The combined organic phases were dried over anhydrous $MgSO_4$ and then filtered. The organic solvent was evaporated under vacuum and the residue was purified by silica gel column chromatography, using a mixture of hexane and ethyl acetate (4:1) as eluent to give the compound **1**.

Yield: 65%. IR (KBr) cm^{-1}: 3395, 3030, 2961, 1493, 1452, 1217, 1061, 991, 761. ^1H NMR (200 MHz, $CDCl_3$): 7.33–7.33 (m, 5H), 4.89 (dd, 1H, *J* = 3.4 Hz, 9 Hz), 3.67–3.48 (m, 2H), 2.46 (s, 1H). ^{13}C NMR (50 MHz): 140.3, 128.5, 128.3, 125.9, 73.7, 39.9 MS, *m*/*z* (relative intensity): 200–202 (M+2) (3), 121 (1), 107 (100), 91 (6), 79 (51), 65 (4), 51 (15).

3.3. Synthesis of (RS)-1-bromo-2-acetoxy-2-(phenyl)ethane (**2**)

In an one-necked round-bottomed flask, (*RS*)-2-bromo-1-(phenyl)ethanol **1** (207 mg, 1.03 mmol) was dissolved in dichloromethane (2.5 mL) with triethylamine (0.42 mL, 3.1 mmol), DMAP (4-*N*,*N*-dimethylaminopyridine; 6.32 mg, 0.052 mmol) and acetic anhydride (0.3 mL, 3.1 mmol). The mixture was stirred at room temperature (25 °C) for 24 h. After this period, water (10 mL) was added to the mixture. The resulting solution was extracted with CH_2Cl_2 (3× 10 mL). The combined organic phases were dried over anhydrous $MgSO_4$ and then filtered. The organic solvent was evaporated under vacuum and the residue was purified by silica gel column chromatography, using a mixture of hexane and ethyl acetate (9:1) as eluent to give the compound **2**.

Yield: 90%. IR (KBr) cm^{-1}: 2937, 1604, 1447, 1374, 1219, 1084, 997, 967. ^1H NMR (200 MHz, $CDCl_3$): 7.37–7.34 (m, 5H), 6.01–5.94 (m, 1H), 3.65–3.59 (m, 2H), 2.13 (s, 3H). ^{13}C NMR (50 MHz): 171.8, 137.6, 128.2, 129.3, 125.9, 73.6, 36.6, 21.0. MS, *m*/*z* (relative intensity): 243 (0.45), 241 (1.22), 118 (4.8), 105 (100), 91 (2.84), 77 (41), 65 (1.98), 51 (15.79).

3.4. Synthesis of Fe_3O_4 nanoparticles

Superparamagnetic nanoparticles of magnetite were obtained by co-precipitation method [44]. To protect the oxidation of the nanoparticles, water (Milli-Q) was deoxygenated by a flow of N_2 and the reaction was maintained under N_2 atmosphere. A aqueous solution of Fe^{2+} and Fe^{3+} mixed oxides (0.1 and 0.2 mol/L, respectively) was slowly dropped into a solution of NaOH (0.5 M). The reaction was maintained under mechanical stirrer (2000 rpm) for 30 minutes. After this period, the black suspension was washed several times with water until reach pH 7.

The black suspension was washed with methanol (3× 10 mL) with a help of an external magnetic field. This suspension was dispersed in 70 mL of toluene/methanol mixture (1:1) and heated at 95 °C under N_2 atmosphere until the evaporation of 50% of the solu-

tion volume. After the evaporation, 35 mL of methanol was added and the mixture was re-evaporated to one-half. This procedure was repeated three more times and then, the magnetic nanoparticles used for surface functionalization.

3.5. Functionalization of magnetic nanoparticles

3.5.1. Preparation of amine-functionalized magnetic nanoparticles (APTS-MagNP)

The γ-aminopropyltriethoxysilane was added to the magnetic nanoparticles (0.2 mL/1 mg magnetic nanoparticles). The suspension was heated under N_2 and refluxed at 110 °C through 12 h. The suspension was washed with methanol (10× 10 mL) and ethanol (10× 10 mL), and then the amine-functionalized magnetic nanoparticles were dried under vacuum for 24 h.

In order to confirm the coating of the magnetite surface through the silanization reaction, an FTIR spectrum of the APTES-magnetite was obtained [27].

3.5.2. Preparation of carboxybenzaldehyde-functionalized magnetic nanoparticles (Carboxy-APTS-MagNP)

In a three-necked round-bottomed flask, were added amine-functionalized magnetic nanoparticles (500 mg) and a solution of TBME and ethanol (1:1, 500 mL). The solution was cooled to 0 °C and carboxybenzaldehyde (6.5 g) was added with a solution of *tert*-butyl methyl ether (TBME) and ethanol (1:1, 500 mL). The solution was stirred for 4 h at 0 °C. After this period, the carboxy-imine-functionalized magnetic nanoparticles were washed with TBME (50 mL) and dried under vacuum for 24 h.

Carboxy-imine-functionalized magnetic nanoparticles (20 mg), $NaBH_4$ (10 mg) and benzoic acid (24 mg) were ground for 1 h in an agate mortar and a pestle at room temperature. Then, the particles were washed with saturated aqueous solution of sodium bicarbonate (1 mL) and TBME (1 mL), and dried under vacuum for 6 h to give the carboxy-amino-functionalized magnetic nanoparticles.

In an Erlenmeyer flask containing 20 mg of this complex, were added 5 mL of EDC solution [5% v/v; 1-ethyl-3-(3-dimethyl aminopropyl) carbodiimide hydrochloride]. This mixture was sonicated at 25 °C during 10 min. After this period, the magnetic nanoparticles were washed with phosphate buffer solution (pH 7, 100 mM, 3× 10 mL) and then used for lipase immobilization.

3.5.3. Preparation of glutaraldehyde-functionalized magnetic nanoparticles (GLU-APTS-MagNP)

In a 2 mL microtube (*eppendorff*®) containing 20 mg of amine-functionalized magnetic nanoparticles (APTS-MagNP) were added 25 μL of aqueous solution of glutaraldehyde (25% v/v). The mixture was stirred at 25 °C and 800 rpm for 2 h. After this period, the black material with strong magnetization was recovered. The glutaraldehyde-functionalized magnetic nanoparticles were used for the lipase immobilization.

3.5.4. Preparation of a B. cepacia lipase aqueous solution

In a 15 mL Falcon tube were added 100 mg of *B. cepacia* lipase and 1 mL of phosphate buffer solution (pH 7, 100 mM) followed by centrifugation at 6000 rpm for 15 min to remove insoluble components. The supernatant solution was recovered and the UV absorption value of the solution was measured at 595 nm to calculate the protein concentration by Bradford method.

3.6. Protein determination

The protein content was determined by Bradford method [28]. For accurate calculation of the immobilized lipase, a calibration curve was obtained at 595 nm by the use of bovine serum albumin (BSA) as standard protein solution in different concentrations.

After the immobilization process, the magnetic nanoparticles were retained by a magnet and, 100 μL of the supernatant solution was collected and added 3 mL of Bradford reagent. After 3 min the value of absorbance at 595 nm was obtained and compared with a calibration curve to calculate the amount of immobilized lipase on magnetic nanoparticles.

3.7. General method for lipase immobilization

In a 2 mL microtube (*eppendorff*®) containing 20 mg of functionalized magnetic nanoparticles were added 1 mL of enzymatic solution (0.55 mg lipase/mL). The mixture was stirred at 32 °C and 800 rpm for 1 h. The immobilized lipase was recovered magnetically and washed with a phosphate buffer solution (3× 100 μL, pH 10, 100 mM). The protein content in the supernatant was measured by Bradford method [28].

3.8. Enzymatic kinetic resolution of (RS)-2-bromo-1-(phenyl)ethanol (**1**)

In a 2 mL microtube (*eppendorff*®) containing 20 mg of magnetic nanoparticles with immobilized lipase by appropriate methodology (see Tables 1–3), (*RS*)-2-bromo-1-(phenyl)ethanol (0.01 mmol) and vinyl acetate (0.3 mmol) were dispersed in toluene or TBME and stirred at appropriate temperature (see Tables 1–3) for appropriate time (see tables) under 800 rpm.

3.9. GC analysis for determination of the enantiomeric excess

The enantiomeric excesses of (*RS*)-2-bromo-1-(phenyl)ethanol (**1**) and the product (*RS*)-1-bromo-2-acetoxy-2-(phenyl)ethane (**2**) were analyzed by GC/FID in a chiral capillary column (Chirasil-Dex CB-Varian). GC conditions: Injector 220 °C; detector: 220 °C; pressure: 100 kPa. Column temperature: 110 °C, 1 °C/min up to 135 °C. Retention times for (*RS*)-2-bromo-1-(phenyl)ethanol (**1**): [(*R*)-**1** = 19.2 min, (*S*)-**1** = 20.0 min]. (*RS*)-1-bromo-2-acetoxy-2-(phenyl)ethane (**2**): [(*R*)-**2** = 14.2 min, (*S*)-**2** = 15.2 min].

3.10. Absolute configuration

The absolute configuration of 2-bromo-1-(phenyl)ethanol and 1-bromo-2-acetoxy-2-(phenyl)ethane was determined by comparison of the sign of the measured specific rotation with those of the literature [45].

Acknowledgements

The authors thank FAPESP and CNPq for financial support. The authors acknowledge the support from FAPESP, CNPq, and PETROBRAS, and Professor Pedro K. Kyohara (Institute of Physics, Univ. S. Paulo) for obtaining TEM images of APTS-MagNP.

References

[1] P. Berglund, Biomol. Eng. 18 (2001) 13.
[2] D.L. Hughes, J.J. Bergan, J.S. Amato, M. Bhupathy, J.L. Leazer, J.M. McNamara, D.R. Sidler, P.J. Reider, E.J.J. Grabowski, J. Org. Chem. 55 (1990) 6252.
[3] A. Ghanem, Tetrahedron 63 (2007) 1721.
[4] A. Ghanem, H.Y. About-Enein, Tetrahedron: Asymmetry 15 (2004) 3331.
[5] V. Gotor-Fernandez, E. Busto, V. Gotor, Adv. Synth. Catal. 348 (2006) 797.
[6] V. Gotor-Fernández, R. Brieva, V. Gotor, J. Mol. Catal. B: Enzym. 40 (2006) 111.
[7] M. Mekrami, S. Sicsic, Tetrahedrom: Asymmetry 3 (1992) 431.
[8] M. Ono, Y. Ogura, K. Hatogai, H. Akita, Chem. Pharm. Bull. 49 (2001) 1581.
[9] E. Santaniello, P. Ferraboschi, P. Grisenti, Enzyme Microb. Technol. 15 (1993) 367.
[10] M.I. Youshko, F. van Rantwijk, R.A. Sheldon, Tetrahedron: Asymmetry 12 (2001) 3267.
[11] S.-H. Huang, M.-H. Liao, D.-H. Chen, Biotechnol. Prog. 19 (2008) 1095.
[12] A. Ito, M. Shinkai, H. Honda, T. Kobayashi, J. Biosci. Bioeng. 100 (2005) 1.

[13] J. Kim, J.W. Grate, P. Wang, Chem. Eng. Sci. 61 (2006) 1017.
[14] P. Tartaj, M.P. Morales, T. González-Carreño, S. Veintemillas-Verdaguer, C.J. Serna, J. Magn. Magn. Mater. 290 (2005) 28.
[15] A. Johnson, A.M. Zawadzka, L.A. Deobad, R.L. Crawford, A.J. Paszczynski, J. Nanopartic. Res. 10 (2008) 1009.
[16] R.E. Fernandez, E. Bhattacharya, A. Chadha, Appl. Surf. Sci. 254 (2008) 4512.
[17] S.-Y. Shaw, Y.-J. Chen, J.-J. Ou, L. Ho, Enzyme Microb. Technol. 39 (2006) 1089.
[18] J.M. Palomo, R.L. Segura, G. Fernandez-Lorente, R. Fernandez-Lafuente, J.M. Guisan, Enzyme Microb. Technol. 40 (2007) 704.
[19] S. Maury, P. Buisson, A. Perrard, A.C. Pierre, J. Mol. Catal. B: Enzym. 32 (2005) 193.
[20] P. Hara, U. Hanefeld, L.T. Kanerva, J. Mol. Catal. B: Enzym. 50 (2008) 80.
[21] P. Hara, U. Hanefeld, L.T. Kanerva, Green Chem. 11 (2009) 250.
[22] T. Itoh, S. Han, Y. Matsushida, S. Hayase, Green Chem. 6 (2004) 437.
[23] Y. Zhang, J. Li, D. Han, H. Zhang, P. Liu, C. Li, Biochem. Biophys. Res. Commun. 365 (2008) 609.
[24] P. Kumar, R.K. Upadhyay, R.K. Pandey, Tetrahedron: Asymmetry 15 (2004) 3955.
[25] E.J. Corey, G.A. Reichard, Tetrahedron Lett. 30 (1989) 5207.
[26] D.D. Wirth, M.S. Miller, S.K. Boini, T.M. Koenig, Org. Process Res. Dev. 4 (2000) 513.
[27] C.G.C.M. Netto, L.H. Andrade, H.E. Toma, Tetrahedron: Asymmetry 20 (2009) 2299.
[28] M.M. Bradford, Anal. Biochem. 72 (1976) 248.
[29] J.D. Schrag, Y. Li, M. Cygler, D. Lang, T. Burgdorf, H.J. Hecht, R. Schmid, D. Schomburg, T.J. Rydel, J.D. Oliver, L.C. Strickland, C.M. Dunaway, S.B. Larson, J. Day, A. McPherson, Structure 5 (1997) 187.
[30] R.C. Weast, Handbook of Chemistry and Physics, 67th ed., CRC Press, FL, USA, 1986.
[31] R.D. Waldron, Phys. Rev. 99 (1955) 1727.
[32] M. Ma, Y. Zhang, W. Yu, H.-Y. Shen, H.-Q. Zhang, N. Gu, Colloids Surf. A 212 (2003) 219.
[33] L. Guang-She, L. Li-Ping, R.L. Smith Jr., H. Inomata, J. Mol. Struct. 560 (2001) 87.
[34] S. Bruni, F. Cariati, M. Casu, A. Lai, A. Misunu, G. Piccaluga, S. Solinas, Nanostruct. Mater. 11 (1999) 573.
[35] L.D. White, C.P. Tripp, J. Colloids Interface Sci. 232 (2000) 400.
[36] Z. Xu, Q. Liu, J.A. Finch, Appl. Surf. Sci. 120 (1997) 269.
[37] S. Ramesh, I. Felner, Y. Koltypin, A. Gedanken, J. Mater. Res. 15 (2000) 944.
[38] B. Stuart, Infrared Spectroscopy: Fundamentals and Applications, John Wiley & Sons Ltd., Chichester, UK, 2004.
[39] L. Fei, S. Perrett, Int. J. Mol. Sci. 10 (2009) 646.
[40] C.S. Chen, Y. Fujimoto, G. Girdaukas, C.J. Sih, J. Am. Chem. Soc. 104 (1982) 7294.
[41] A.J.J. Straathof, J.A. Jongejan, Enzyme Microb. Technol. 21 (1997) 559.
[42] C. Mateo, J.M. Palomo, G. Fernandez-Lorente, J.M. Guisan, R. Fernandez-Lafuente, Enzyme Microb. Technol. 40 (2007) 1451.
[43] R.A. Sheldon, Adv. Synth. Catal. 349 (2007) 1289.
[44] M.C. Yamaura, R.L. Camilo, L.C. Sampaio, M.A. Macedo, M. Nakamura, H.E. Toma, J. Magn. Magn. Mater. 279 (2004) 210.
[45] A. Goswami, J. Goswami, Tetrahedron Lett. 46 (2005) 4411.